

Supplementary Information

Assessing the Suitability of Iron Tungstate (Fe_2WO_6) as a Photoelectrode Material for Water Oxidation

Fatwa F. Abdi*, Abdelkrim Chemseddine, Sean P. Berglund and Roel van de Krol

Helmholtz-Zentrum Berlin für Materialien und Energie GmbH, Institute for Solar Fuels, Hahn-Meitner-Platz 1, 14109 Berlin, Germany

* Correspondence: fatwa.abdi@helmholtz-berlin.de

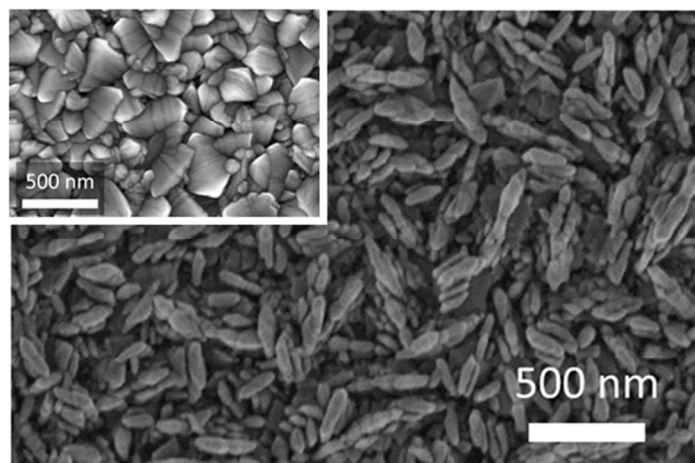


Figure S1. Scanning electron micrograph (SEM) of Fe_2WO_6 thin film deposited on FTO at 500 °C. The inset (upper left corner) shows the SEM of the FTO substrate for comparison.

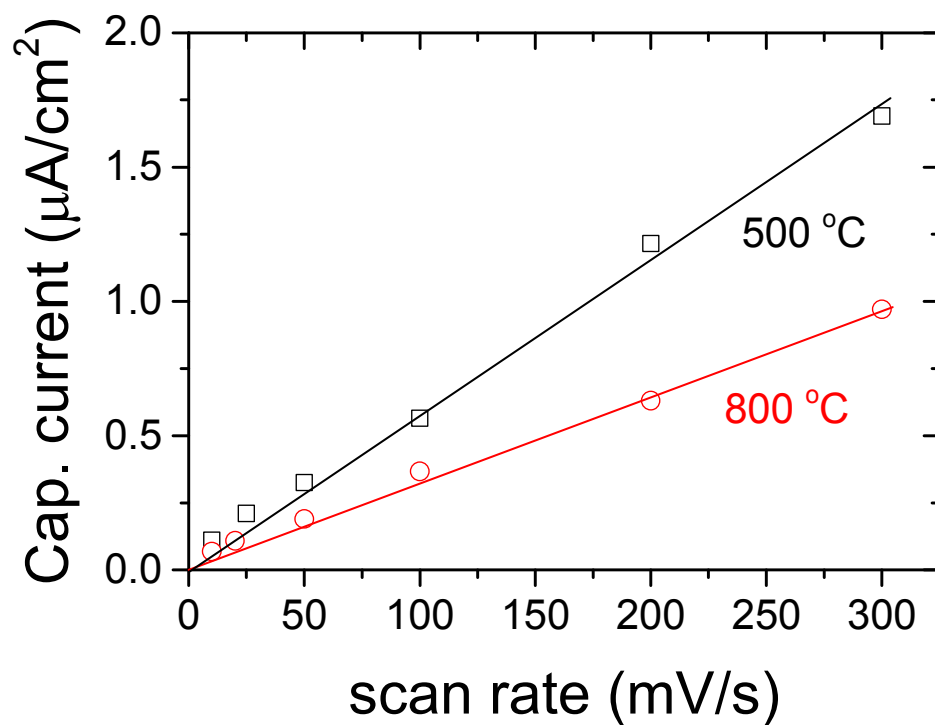


Figure S2. Capacitive current density of the as-deposited (500 °C, black) and annealed (800 °C, red) Fe_2WO_6 films as a function of the potential scan rate. The ratio of the slope of these curves represents the ratio of the electrochemical active area of the films.

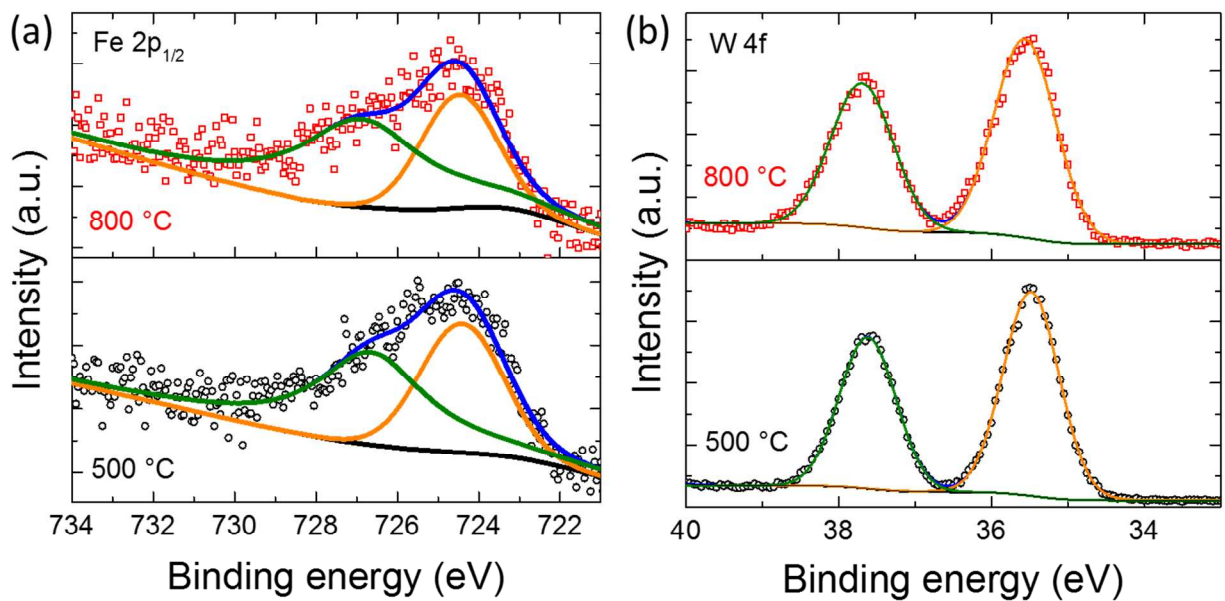


Figure S3. X-ray photoelectron spectra of Fe_2WO_6 thin films as-deposited at 500 °C and annealed at 800 °C. The spectra of (a) $\text{Fe } 2p_{1/2}$ and (b) $\text{W } 4f$ core levels are shown.

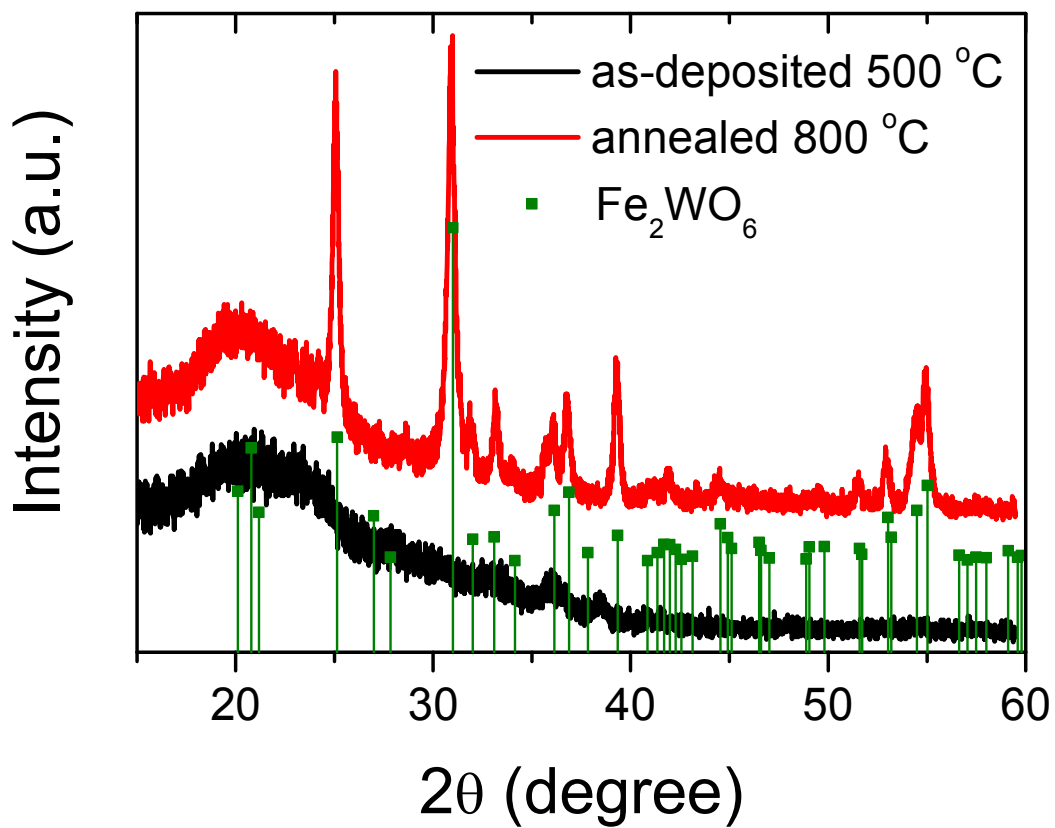


Figure S4. X-ray diffraction spectra for the as-deposited (black) and annealed (red) Fe₂WO₆ films deposited on quartz substrate.

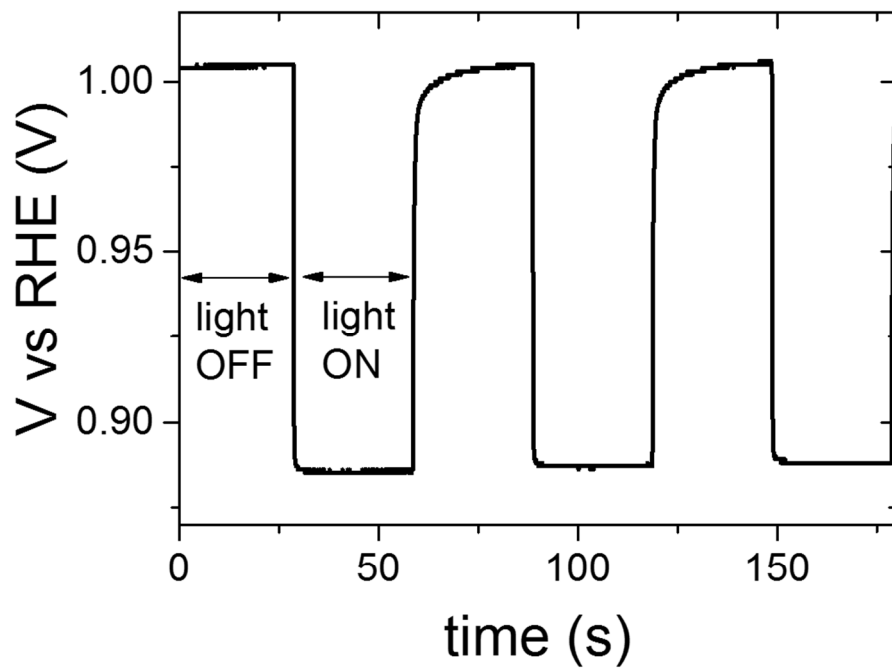


Figure S5. Open circuit potential of Fe_2WO_6 thin film annealed at $800\text{ }^\circ\text{C}$ under chopped AM1.5 illumination. $0.1\text{ M H}_2\text{O}_2$ is added to the potassium hydroxide electrolyte to better define the redox potential.

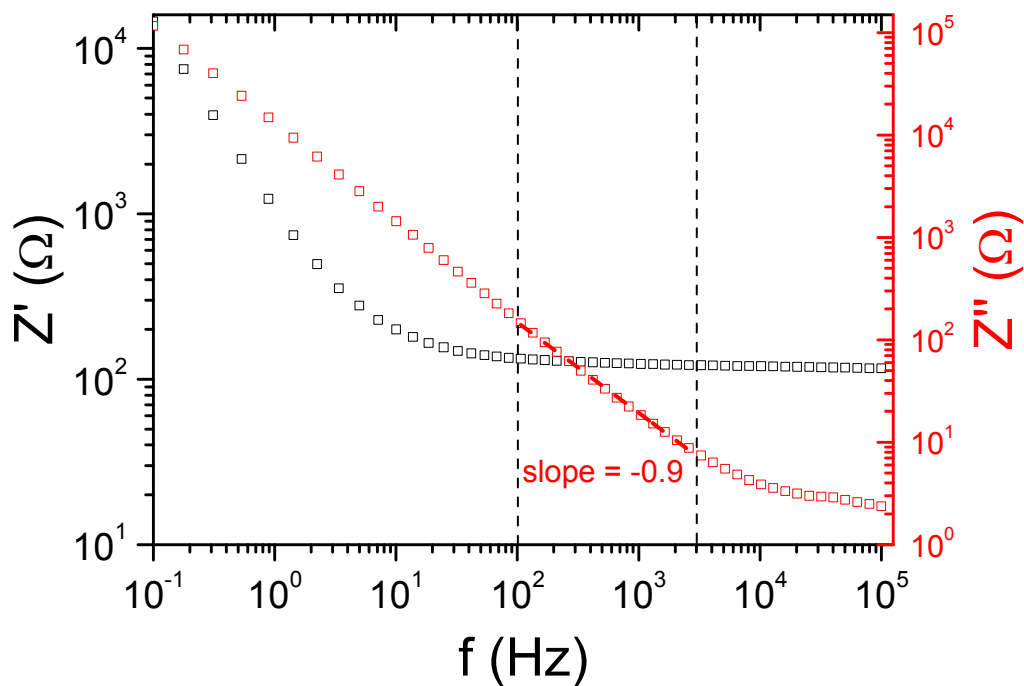


Figure S6. Log-log plot of real and imaginary impedance as a function of frequency of potential modulation of the as-deposited Fe_2WO_6 film, at applied potential of 1.0 V vs RHE. The Mott-Schottky analysis assumes that the real impedance is independent of frequency and the imaginary impedance is linearly dependent of frequency with a slope of -1 (or as close as possible). This condition is somewhat satisfied for our films at frequency range of 100-3000 Hz.

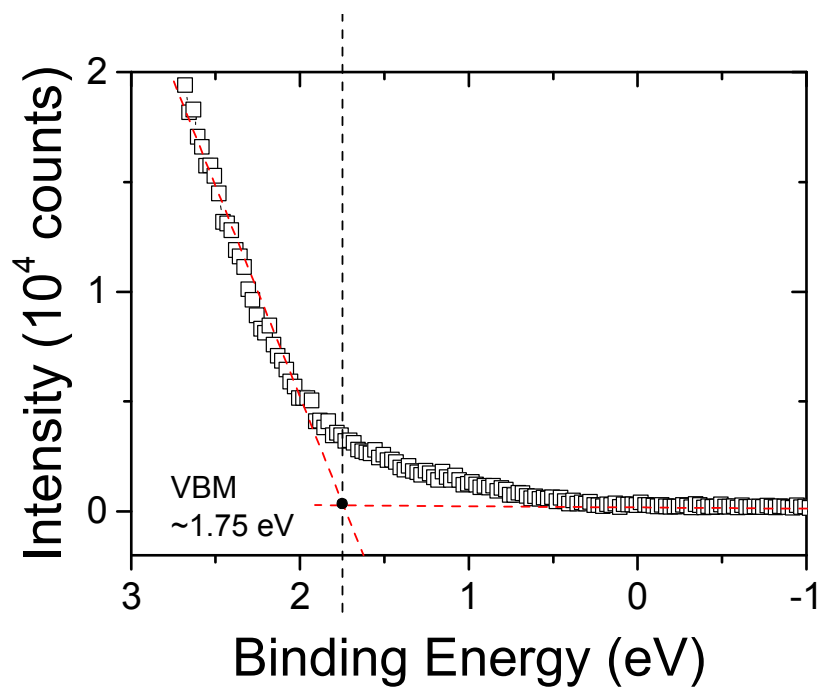


Figure S7. Ultraviolet photoelectron spectroscopy (UPS) spectrum of the annealed (800 °C) Fe_2WO_6 film. The valence band maximum is estimated to be located at 1.75 ± 0.15 eV below the Fermi level (represented by zero binding energy).

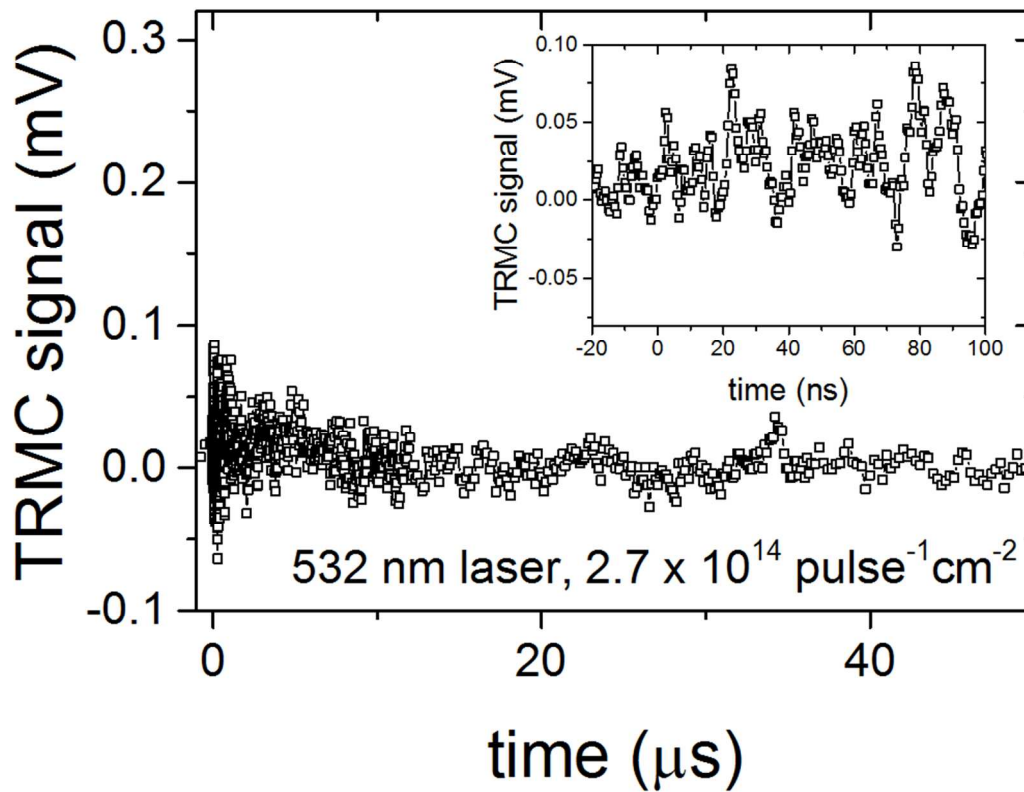


Figure S8. Time-resolved microwave conductivity (TRMC) signal of the Fe_2WO_6 thin films. The illumination was performed with a 532 nm Nd:YAG laser, with an intensity of $2.7 \times 10^{14} \text{ pulse}^{-1} \text{ cm}^{-2}$. The inset shows the magnification of the early time-window (up to 100 ns). The fact that no noticeable signal is detected indicates that the carrier lifetime in our Fe_2WO_6 films is faster than 1 ns (the resolution of our TRMC setup).

Supplementary note 1: IMPS theory

Intensity modulated photocurrent spectroscopy (IMPS) uses modulation of the light intensity to probe the rate of reactions involving photo-generated carriers. A simplified model is then used to unravel the competition between hole transfer and surface recombination at the semiconductor-electrolyte interface (see Figure S9a). IMPS can therefore provide insights into the processes at this interface under illumination and applied bias.

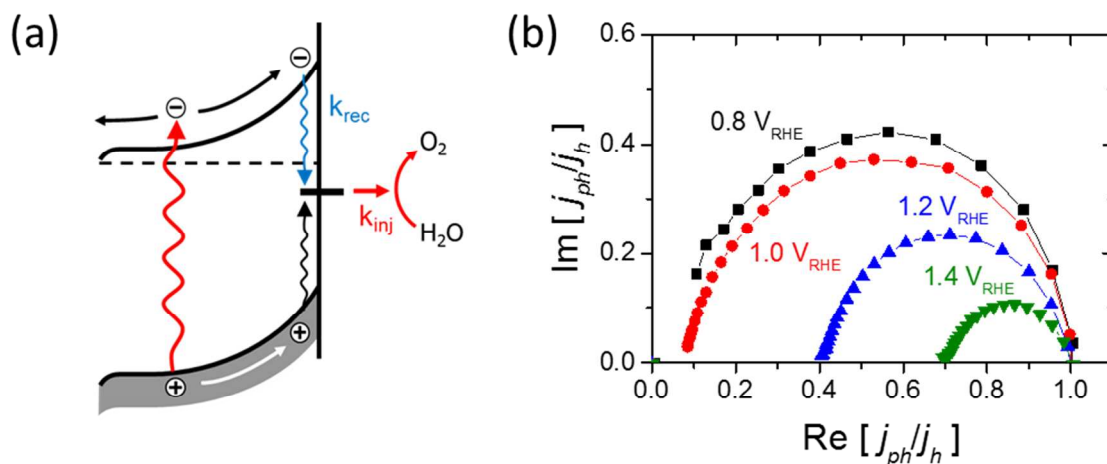


Figure S9. (a) Simplified model of the elementary processes in a semiconductor (an n-type semiconductor is shown here). Upon illumination, photo-excited carriers move towards the semiconductor-electrolyte interface, where either charge injection (k_{inj}) or recombination (k_{rec}) takes place under reverse bias. In this model, charge injection is depicted to occur via surface states. (b) IMPS spectra (imaginary vs. real photocurrent response) of our Fe_2WO_6 film under different applied bias potentials. The frequency of the modulation is increasing in clockwise direction.

As a result of the sinusoidal modulations of the light intensity, the same modulation of the photocurrent is observed. The modulated photocurrent response consists of the hole current (minority carrier) and the electron current (majority carrier). The electron current is lagging behind the hole current with the opposite sign, causing in-phase and out-of-phase components of the photocurrent response. This results in a semicircle, when plotted in a complex plane, as shown in Fig. S9b. The imaginary photocurrent reaches a maximum when the frequency matches the characteristic relaxation constant of the system.

$$\omega_{\max} = k_{inj} + k_{rec} \quad (S1)$$

Here, k_{inj} and k_{rec} are the first order charge transfer and recombination rate constants (s^{-1}), respectively. The high and low frequency intercepts of the x-axis (imaginary current = 0) correspond to the spike and steady state photocurrents in a transient photocurrent experiment, respectively. At the high frequency intercept, the recombination is “frozen” due to fast modulation, which means the measured current is equal to the hole current (the intercept is one when the photocurrent is normalized with respect to the hole current, as shown in Fig. S9b). The low frequency intercept then represents the fraction of the flux of the transferred holes to the overall surface processes (both hole transfer and recombination). This is also called the charge transfer efficiency,

$$\eta_{CT} = \frac{k_{inj}}{k_{inj} + k_{rec}} \quad (S2)$$

The individual reaction rates (k_{inj} and k_{rec}) can then be calculated from equations S1 and S2.

It is important to note that the model is based on several assumptions. First, bulk processes (e.g. bulk recombination, trapping) are invisible, and only surface processes occur within the timescale of the measurement (sub-ms to s). Second, no changes in band bending occur during the modulated illumination. This means that the intensity of applied modulation is too small to significantly influence the space charge capacitance and the density of majority carriers. These assumptions are usually easy to fulfil, since the frequency (mHz-kHz) and intensity of the light modulation can be adjusted accordingly.

Supplementary note 2: The effect of surface state density to photocurrent-voltage curve

We use a modified Gärtner equation initially reported by Peter et al. [39,40] in order to evaluate the influence of surface state recombination to the photocurrent-voltage curve. In brief, the photocurrent consists of two components. First, the flux of minority carriers into the surface if recombination in the space charge layer can be neglected is given by the Gärtner equation:

$$g = \phi_0 \left[1 - \frac{e^{-\alpha W}}{1 + \alpha L} \right] \quad (\text{S3})$$

where ϕ_0 is the incident photon flux, α is the absorption coefficient (see Eq. 1 in the manuscript), W is the width of the space charge layer (see Eq. 5 in the manuscript), and L is the minority carrier diffusion length. The surface state recombination current at any given time, $j_{ss}(t)$, is then influenced by the surface concentration of majority carriers (n_s), the rate constant for the capture of majority carriers (k_n), the surface state density (N_{SS}), and the change in occupancy of the surface state, $\Delta f(t)$, according to the following equation:

$$j_{ss}(t) = k_n n_s N_{ss} \Delta f(t) \quad (\text{S4})$$

$$n_s = n_0 \exp\left(\frac{-q(V_{appl} - V_{FB})}{kT}\right) \quad (\text{S5})$$

n_0 is the equilibrium majority carrier density in the bulk, V_{appl} is the applied potential, V_{FB} is the flatband potential, k is Boltzmann's constant, and T is the temperature. The steady-state photocurrent is then defined as:

$$j_{photo}(\infty) = g - k_n n_s N_{ss} \Delta f(\infty) \quad (S6)$$

$$\Delta f(\infty) = f_\infty - f_0 \quad (S7)$$

where f_∞ is the surface state occupancy under steady-state illumination and f_0 is the surface state occupancy in the dark. Both occupancies can be calculated as follows:

$$f_0 = \left[1 + \exp\left(\frac{E_{SS} - q(V_{appl} - V_{FB})}{kT}\right) \right] \quad (S8)$$

E_{SS} is the energy level of the surface state relative to the conduction band.

$$f_\infty = \left(-B - \sqrt{B^2 - 4AC} \right) \quad (S9)$$

where:

$$A = k_p k_n n_s N_{SS}^2 \quad (S10)$$

$$B = -\left[k_p N_{SS} g + k_p k_n n_s N_{SS}^2 (1 + f_0) + k_{inj} k_n n_s N_{SS} \right] \quad (S11)$$

$$C = k_p N_{SS} g + k_p k_n n_s N_{SS}^2 f_0 + k_{inj} k_n n_s N_{SS} \quad (S12)$$

k_p is the rate constant for the capture of minority carrier.

Figure S10 is the calculated normalized photocurrent (j_{photo}/ϕ_0) as a function of applied potential, according to Eq. S6. The effect of varying surface state density is shown as a cathodic shift of the curve. The following constants are used for the simulation: $\alpha = 3.3 \times 10^4 \text{ cm}^{-1}$, $k_n = 10^{-7} \text{ cm}^3 \text{ s}^{-1}$, $k_p = 10^{-8} \text{ cm}^3 \text{ s}^{-1}$, $n_0 = 10^{20} \text{ cm}^{-3}$, $\epsilon_r = 410$, $L = 1 \text{ nm}$, and $E_{SS} = 0.3 \text{ eV}$.

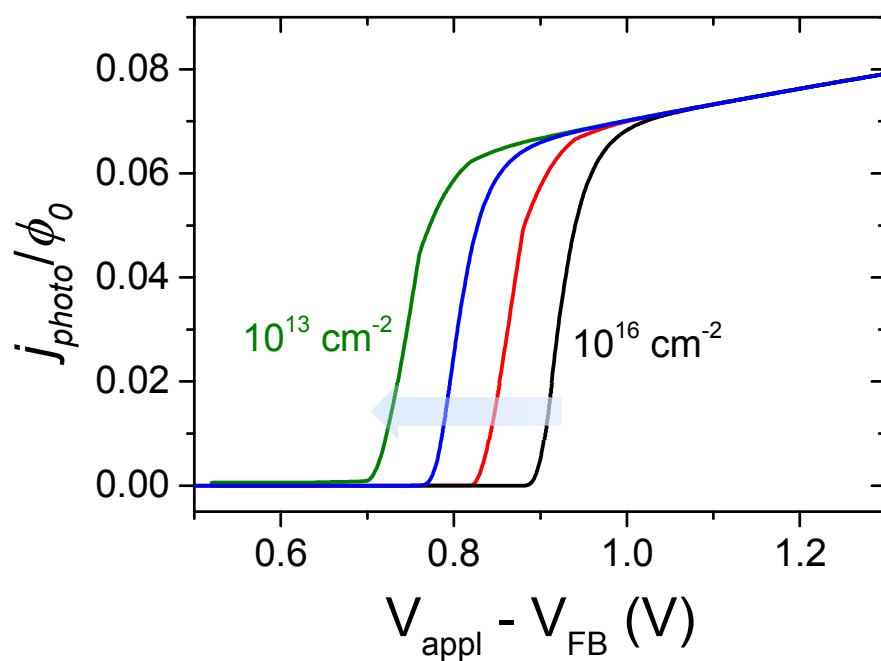


Figure S10. Normalized photocurrent as a function of bias potential, calculated for different surface state concentrations, based on the model described in references [39,40]. As the surface state concentration decreases, the onset potential shifts cathodically.